Diffuse optical signals in response to peripheral nerve stimulation reflect skeletal muscle kinematics

M. Kelley Erb,[1,]* Debbie K. Chen,[2] Angelo Sassaroli,[2] Sergio Fantini,[2] and Peter R. Bergethon[1]

[1]*Boston University School of Medicine, Department of Anatomy & Neurobiology, Boston MA, USA*
[2]*Tufts University, Department of Biomedical Engineering, Medford MA, USA*
*kerb@bu.edu

Abstract: Previously we have reported a near-infrared optical response in the region occupied by a peripheral nerve that is distal to the site of electrical stimulation of that peripheral nerve. This "intermediate" signal is vascular in nature but its biological origin not been elucidated. In the present study, an animal model of the signal has been created and our human studies expanded to directly investigate the contribution of non-artifactual vascular motion induced by muscle contraction to the biological origin of this signal. Under non-invasive conditions during stimulation of the exposed sciatic nerve of the Sprague-Dawley rat, optical responses are robust. These signals can be abolished both pharmacologically and surgically using methods that eliminate muscle motion while leaving the electrophysiological health of the nerve intact. In human studies, signals that are elicited on stimulation of nerves containing motor axons, both within and outside the predicted imaging volume of the spectrometer, have similar temporal characteristics of those previously observed. Moreover, stimulation of sensory nerves alone does not elicit an optical response. These results strongly suggest that the intermediate signals are derived from stimulus-induced muscle contraction (whether via an innervating nerve or by direct stimulation) causing translational vascular motion within the optically interrogated region.

OCIS codes: (170.0170) Medical optics and biotechnology; (170.3890) Medical optics instrumentation; (170.6510) Spectroscopy; tissue diagnostics.

References and links

1. Y. Tong, J. M. Martin, A. Sassaroli, P. R. Clervil, P. R. Bergethon, and S. Fantini, "Fast optical signals in the peripheral nervous system," J. Biomed. Opt. **11**(4), 044014 (2006).
2. D. K. Chen, Y. Tong, A. Sassaroli, P. R. Bergethon, and S. Fantini, "Fast optical response to electrical activation in peripheral nerves - art. no. 643104," Multimodal Biomedical Imaging II **6431**, 43104–43104 43100 (2007).
3. S. Fantini, D. K. Chen, J. M. Martin, A. Sassaroli, and P. R. Bergethon, "Near-infrared signals associated with electrical stimulation of peripheral nerves," Proc SPIE **7174** (2009).
4. J. Steinbrink, F. C. Kempf, A. Villringer, and H. Obrig, "The fast optical signal--robust or elusive when non-invasively measured in the human adult?" Neuroimage **26**(4), 996–1008 (2005).
5. D. K. Chen, M. K. Erb, Y. Yu, A. Sassaroli, P. R. Bergethon, and S. Fantini, "Spectral and Spatial Features of Diffuse Optical Signals in Response to Peripheral Nerve Stimulation," submitted.
6. S. Virmani, D. K. Tempe, V. Datt, A. S. Tomar, A. Banerjee, H. S. Minhas, and S. Goel, "Effect of muscle relaxants on heart rate, arterial pressure, intubation conditions and onset of neuromuscular block in patients undergoing valve surgery," Ann. Card. Anaesth. **9**(1), 37–43 (2006).
7. A. Esmaoglu, A. Akin, A. Mizrak, Y. Turk, and A. Boyaci, "Addition of cisatracurium to lidocaine for intravenous regional anesthesia," J. Clin. Anesth. **18**(3), 194–197 (2006).
8. S. Fantini, M. A. Franceschini, J. B. Fishkin, B. Barbieri, and E. Gratton, "Quantitative-Determination of the Absorption-Spectra of Chromophores in Strongly Scattering Media - a Light-Emitting-Diode Based Technique," Appl. Opt. **33**(22), 5204–5213 (1994).

9. S. Fantini, M. A. Franceschini, and E. Gratton, "Semi-Infinite-Geometry Boundary-Problem for Light Migration in Highly Scattering Media - a Frequency-Domain Study in the Diffusion-Approximation," J. Opt. Soc. Am. B **11**(10), 2128–2138 (1994).
10. V. Quaresima, M. A. Franceschini, S. Fantini, E. Gratton, and M. Ferrari, "Difference in leg muscles oxygenation during treadmill exercise by a new near infrared frequency-domain oximeter," Photon Propagation in Tissues Iii, Proceedings Of **3194**, 116–120532 (1998).
11. H. L. Liu, D. A. Boas, Y. T. Zhang, A. G. Yodh, and B. Chance, "A simplified approach to characterize optical properties and blood oxygenation in tissue using continuous near infrared," Optical Tomography, Photon Migration, and Spectroscopy of Tissue and Model Media: Theory, Human Studies, and Instrumentation, Proceedings of, Pts 1 and 2 **2359**, 496–502880 (1995).
12. C. Chen, N. Yamaguchi, and F. Varin, "Dose-dependency of pharmacokinetic/pharmacodynamic parameters after intravenous bolus doses of cisatracurium," Br. J. Anaesth. **101**(6), 788–797 (2008).
13. F. Buchthal, and H. Schmalbruch, "Contraction times and fibre types in intact human muscle," Acta Physiol. Scand. **79**(4), 435–452 (1970).
14. R. Close, "Dynamic Properties of Fast and Slow Skeletal Muscles of the Rat during Development," J. Physiol. **173**, 74–95 (1964).

1. Introduction

Previously, we have reported a non-invasively recorded optical response that is both co-localized with the peripheral nerve and correlated to electrical stimulation of that nerve at a site distal to the optical measurement [1]. The optical response is characterized by a change in the tissue diffuse reflectance of 690 and 830 nm light, with a peak latency between 60 and 160 ms and an intensity change on the order of 0.1%. Initial investigations of the sural and median nerves of human subjects revealed that signals were wavelength dependent and exhibited a stimulus-response relationship, increasing in amplitude with increasing stimulus intensity [2,3]. Hemodynamic events have been postulated to underlie the biological origin of these signals on several lines of evidence. First, the measured electrical wave passes under the region of the optical probe within several milliseconds while the timescale of the optical signal is twenty to fifty times longer in latency than the electrical wave and secondly, the presence of a wavelength dependence both suggested that it is changes in absorption rather than scattering that account for this optical signal. The presence of two temporally distinct optical signals are generally well appreciated especially in the context of optical imaging of the brain, one a "fast" signal thought to have a biological origin derived from electric field induced scattering changes in neural tissues and the second a "slow" signal derived from the same biological neurovascular coupling mechanisms that lead to the BOLD signal in functional MRI studies [4]. The non-invasive optical signal that we have described is distinguishable from each of these signals because (1) it was found at the site of the peripheral nervous system and not within the brain, (2) it does not have the temporal or optical characteristics associated with the biological mechanisms of the "fast" signal and, (3) while it has the hemodynamic-derived character of the slower BOLD-type signal it is temporally much faster (on the order of 50 times faster peak latency). For this reason we call this optical signal the "intermediate" optical signal and both this paper and a companion paper found in this volume [5] report on our progress in understanding the biological origins of the intermediate optical signal.

In our companion paper [5] we have shown how the optical characteristics of the intermediate signal suggest translation of blood containing structures within the field of optical interrogation. This leads directly to a search for a causal biological mechanism that might put peripheral-nerve-associated blood vessels into the correct motion to account for the temporal profile of the intermediate signal. Though all of our previous studies have carefully controlled for surface motion artifact to prevent this well known influence on optical signals from contaminating the characterization of the intermediate signal, a logical source for translational mechanical action that could theoretically generate the character of the intermediate signal is the skeletal muscle activated by neuromuscular signaling.

We report here on a study designed using both an animal model and human subjects to directly determine if muscle action acting on structures (tendons, ligaments, soft connective

tissue) in the optical interrogation region co-localized with the nerve and its associated vascular elements might account for the postulated translational motion and contribute to our biological understanding of the source of the intermediate optical signals. An animal model was created using a sciatic nerve preparation of the Sprague-Dawley rat. During proximal stimulation of the exposed nerve, optical responses were measured in a non-contact mode along its distal course before and after both pharmacological and surgical denervation of lower limb muscles. Under both conditions, signals were dramatically reduced or completely eliminated following functional disconnection of the nerve from its muscle. In human subjects, a variety of stimulation and recording configurations were used in the forearm to dissociate: (1) pure motion in the absence of a nerve from (2) pure nerve activation in the absence of motion. The forearm receives motor and sensory innervation from anatomically distinct nerves, providing the opportunity for nerve activation that cannot induce muscle tensioning. This work demonstrates that stimulation of these sensory nerves fails to elicit a signal, whereas the direct induction of motion via stimulation of mixed nerves, both within and outside the imaging volume, generates a large optical response. The responses are consistent with the characteristics of the intermediate optical signal and provide experimental support for the non-artifactual contribution of muscle contraction as a biological factor in the origin for this intermediate signal.

2. Methods

2.1 Electrophysiology

Figures 1 and 2 depict the experimental setups for the animal model and the human subjects, respectively. For both studies, a TECA Synergy nerve conduction velocity (NCV) / electromyography (EMG) monitor (Carefusion Healthcare, San Diego CA) was used to measure sensory nerve action potentials (SNAPs) and compound muscle action potentials (CMAPs).
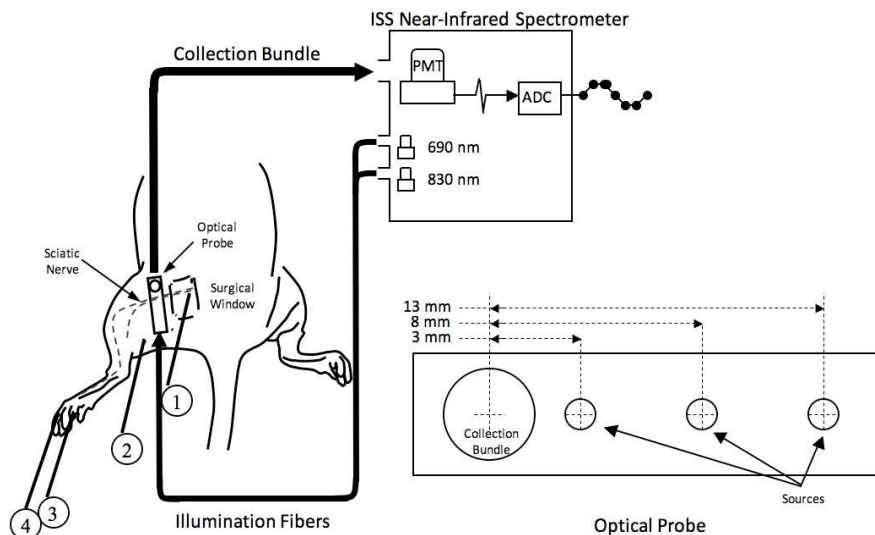

Fig. 1. Experimental setup for the animal model. A surgical window was created over the proximal course of the left sciatic nerve in Sprague-Dawley rats. A non-invasive optical probe delivering 690 and 830 nm light at 3 different source-detector separation distances was coupled to the PMT of a frequency-domain spectrometer and oriented perpendicularly to the course of the nerve. 60 x 600 ms epochs, each synchronized to the delivery of a 0.1 ms current stimulus to the exposed nerve (1), were averaged to generate an optical response. Simultaneously, electrophysiological responses to the stimulus were recorded from the plantar muscles of the left foot. (2) ground electrode, (3) active recording electrode, (4) reference electrode.

In the animal studies, monopolar needle electrodes (Rochester Electromedical, Rochester NY) were used to stimulate the sciatic nerve and to measure CMAPs generated in the plantar muscles of the left foot. A single stimulating electrode was lowered onto the exposed sciatic nerve using a micromanipulator (Narishige USA, East Meadow, NY) while a recording electrode was inserted between interdigital foot-pads II and III. Both the stimulating and recording electrodes were referenced to an electrode inserted in the lateral aspect of digit IV and a common ground placed subcutaneously in the upper leg near the distal 3rd of semitendinosus muscle.

For the human studies, Ag/AgCl electrodes were used to perform a variety of clinical NCV/EMG tests in the forearm, the details of which are described in section 2.4.

2.2 Near-infrared spectrophotometry

Optical measurements at 690 and 830 nm were performed with a commercial near-infrared tissue spectrometer (Imagent, ISS Inc., Champaign, IL) featuring time-multiplexed laser diodes and detection channels based on a photomultiplier tube (PMT). The laser diodes were alternately activated for 5 ms so that each data point represents a 10 ms window of time. The data are thus acquired at a rate of 100 Hz.

For animal studies, the illumination optical train consisted of an Ocean Optics 400 BIF VIS/NIR bifurcated optical fiber coupled, at its bifurcated end, to the laser diodes of the spectrometer and, at its opposite end, to the 600 μm central fiber of an Ocean Optics QR600-VIS-7-125F backscattering/reflectance probe. A 2 mm-diameter collection optical fiber bundle transmitted light from the tissue back to the PMT of the spectrometer. Both the illumination train and the collection bundle were coupled to the animal using a rectangular light block which prevented both from directly contacting the skin and kept illumination light from reaching the detector without first entering the tissue. The optical probe was built so that 3 different distances could separate the illumination fiber and the collection bundle (3 mm, 8 mm, and 13 mm, respectively), shown in Fig. 1.

For the human studies a similar probe was constructed and incorporated into an armband that could be applied to either the proximal or distal forearm. The collection fiber bundle was identical to that used in the animal studies but the illumination train consisted of 2 separate 400 μm-diameter optical fibers. Illumination fibers were coupled to the laser diodes at one end and inserted at a single hole in the light block at the other. As with the animal studies, illumination and detection fibers were held inside the block and off the surface of the skin, so that changes in coupling efficiency between the fibers and the tissue could not contribute to the signals. Source-detector separation for the human probe was 1.5 cm.

A portion of the stimulating electrical pulse was coupled to an auxiliary input of the near-infrared tissue spectrometer to synchronize the electrical stimulation with the acquisition of optical data.

2.3 Animal studies

All surgical procedures were approved by Boston University School of Medicine's Institutional Animal Care and Use Committee. Eight animals were anesthetized using 5% isoflurane and then placed in the prone position on a heated surgical bed and maintained anesthetized with 3% isoflurane. The left hind quarter was shaved using an electric trimmer and a chemical depilator (Nair, Church and Dwight Co., Inc., Princeton, NJ) was used to remove the remaining fur. Once prepared for surgery, isoflurane was discontinued and the animal was given an intraperitoneal injection of Ketamine and Xylazine (90 mg/kg and 4 mg/kg, respectively). The animal was then intubated with a 14-gage intravenous catheter and placed on a TOPO Small Animal Ventilator (Kent Scientific, Torrington, CT) in constant pressure mode with the following parameters: respiratory rate; 50 breaths/min, time ratio of inspiratory phase/total respiratory cycle; 30%, peak inspiratory pressure; 13.5 cmH$_2$O. Blood pressure (BP) and heart rate (HR) were continuously monitored using a common carotid

artery catheter and a transducer flushed with heparinized saline. BP and HR data were amplified with multi-purpose transducer amplifier (Harvard Apparatus, Holliston, MA) and then sampled and displayed using a voltage analog input module controlled by a university serial bus (USB) data acquisition system (National Instruments, cDAQ 9172) and LabView software. Once the animal had stabilized on the ventilator and was non-responsive to foot pinch, a skin incision was made just distal to the sciatic notch, where the anterior head of biceps femoris could be blunt dissected from the caudal margin of gluteus maximus, thus exposing the proximal course of the sciatic nerve. The resulting surgical window was held open using an ophthalmologic speculum.

Optical data were acquired from each source-detector distance during approximately 60 nerve stimulations,. Before each trial, the optical probe was positioned with a micromanipulator so that the source and detector were equidistant and perpendicular to the course of the nerve. After 1 trial at each source detector distance, a 0.2 mg/kg dose of a clinically used neuromuscular blocking agent, Nimbex (Cisatracurium Besylate), was delivered in a 300 µl bolus via the left common carotid artery catheter. CMAPs were then monitored periodically over the next several minutes to track the action of the drug. Once the CMAP was abolished, another set of optical measurements were made at each source-detector separation.

Nimbex belongs to the nondepolarizing class of neuromuscular blocking agents and acts as a competitive antagonist of post-synaptic acetylcholine receptors at the neuromuscular junction. This class of drug has been shown to exhibit affects on the autonomic nervous system [6]. While Nimbex was chosen for its hemodynamic stability [7], a control experiment was necessary to confirm that changes in the signal on delivery of the drug were related to neuromuscular action and not changes in hemodynamic parameters. In an additional set of animals, a second surgical window was made in the popliteal fossa, distal to both the site of stimulation and the placement of the optical probe. Before the start of the experiment, the tibial and common peroneal nerves were mobilized taking care not to damage major vessels in the space. Following the acquisition of data at each source-detector distance, both nerves were cut distal to their blood supply and a second set of data were acquired at each source detector distance.

2.4 Human studies

All human studies were approved by Boston University Medical School's Institutional Review Board. For studies with human subjects, the anatomical locations of the stimulating electrodes, recording electrodes, and the optical probe during each of six experimental conditions (3 sensory and 3 motor) are shown in Fig. 2. To study the effect of motor stimulation, CMAPs were acquired in the abductor pollics brevis (APB) muscle and the abductor digiti minimi (ADM) during stimulation of the median nerve, ulnar nerve, and the recurrent branch of the median nerve. To study the effect of sensory nerve activation, antidromic SNAPs were acquired in the medial antebrachial cutaneous nerve (medAC) and the lateral antebrachial cutaneous nerve (latAC) of 4 subjects while measuring the optical response near the recording electrode. Additionally, in the median nerve, orthodromic SNAPs were acquired at the wrist proximal to the carpal tunnel during stimulation of the proper digital branch of the median nerve in the second digit.

The effect of motor stimulation on optical signals in the wrist was investigated by acquiring compound muscle action potentials using 3 different protocols. In each case, the optical probe was positioned over the space between the tendons of palmaris longus and flexor carpi radialis just proximal to the carpal tunnel. The median nerve runs in this space as it emerges from between muscles of the flexor compartment in the forearm. The recording and reference electrodes were placed adjacent to and on either side of the optical probe and a ground was located on the palmar surface of the hand. Figure 2, panel (a) shows the setup for stimulation of the median nerve along its course at the elbow and measurement of CMAPs

acquired from APB. The recording electrode was located on the muscle belly and a reference placed on the metacarpophalangeal joint of digit I. In a second test, CMAPs were acquired from APB upon stimulation of the recurrent branch of the median nerve in the palm [panel (b)]. Finally, the ulnar nerve was stimulated at the elbow and CMAPs were recorded from ADM [panel (c)]. A recording electrode was placed on the muscle belly and a reference electrode placed on the metacarpophalangeal joint of digit V.
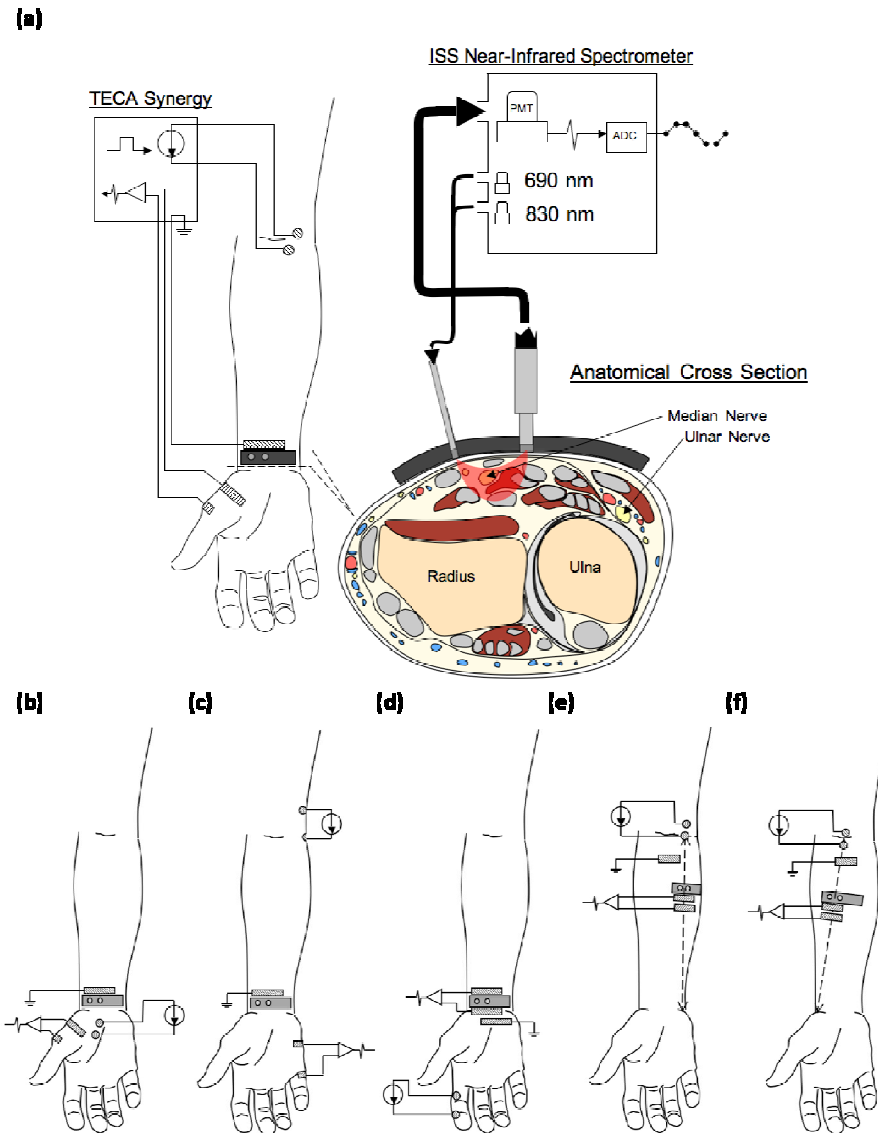
Fig. 2. Experimental setup for the human studies. Myogenic components of the optical response were investigated in human subjects using 6 standard NCV/EMG tests (3 Motor Action Potential tests and 3 Sensory Nerve Action Potential tests). (a) Configuration of the Ag/AgCl electrodes and optical probe while making CMAP measurements of APB during stimulation of the median nerve at the elbow. The anatomical cross section illustrates the location of the median and ulnar nerves in the region of optical interrogation. The probe was positioned to interrogate the median nerve. The configuration of electrodes for investigation of the recurrent branch of the (b) median nerve and (c) ulnar nerve.Optical probe and electrode setup for the (d) median, (e) medial antebrachial cutaneous and (f) lateral antebrachial cutaneous nerves.

Figure 2, panel (d) shows the experimental setup during orthodromic sensory stimulation of the proper digital branch of the median nerve in the second digit while measuring at the wrist. For these tests, the optical probe was in the same position as it had been for the motor testing described above. Figure 2, panels (e) and (f) show the arrangement during stimulation of the medAC and latAC, respectively. For tests of the former, the cathode of the stimulator was placed at the midpoint of an imaginary line connecting the medial epicondyle of the humerus and the tendon of biceps brachii as it crosses the elbow crease. The recording electrode was placed at a point 10 cm distal along a line connecting the stimulator cathode with medial edge of wrist crease. The reference electrode was placed 1 cm distal to the recording electrode and a ground (used for both tests) located between the recording electrode and the stimulator along the midline of the ventral surface of the arm. In tests of the latter, the stimulating electrodes were placed longitudinally and slightly lateral to the midline of the arm, straddling the elbow crease. The recording electrode was located 10 cm distal along a line connecting the midpoint of the elbow crease to the lateral aspect of the wrist. In both tests, optical probe was located proximal and immediately adjacent to the recording electrode, with the sources and detector oriented perpendicular to the nerve.

2.4 Data analysis

The analysis of the optical data has been described previously [5]. Briefly, the relative change in optical irradiance following a single stimulation is expressed as $\delta I_{stim}(t)/I(t_0)$. The average response over N stimulations is then written as $< \delta I_{stim}(t)/I(t_0) >_N = \frac{1}{N} \sum_{i=1}^{N} \delta I_{stim\_i}(t)/I(t_{0i})$.

3. Results

3.1 Animal model

3.1.1 Sciatic nerve stimulation induced optical responses in a rodent model

Figure 3 shows a typical plantar muscle action potential and the corresponding optical time-trace obtained from the middle source-detector separation in the animal model. In general, optical signals obtained from the rodent hind limb are faster than those obtained from the human forearm, reaching peak amplitude between 30 and 40 ms post-stimulus. The amplitude of the signal was on the order of 1-5% and this was not affected by changing the source-detector separation distance. The direction of the signal (positive vs. negative irradiance changes) varied, both within a single animal (at different source-detector separations) or between animals. This finding is in agreement with signals generated in human subjects both in this and previous work [5].
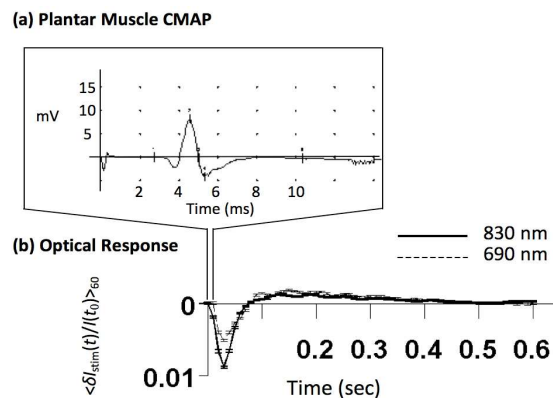

Fig. 3. Typical results from middle source-detector separation in the animal model. (a) A plantar muscle action potential. (b) Signals generated in the lower limb of the Sprague-Dawley rat are faster than signals generated in human subjects.

In the animal model, data were acquired from source-detector pairs separated by multiple distances, an approach that has been used previously [8–11]. Increasing the distance between the source and the detector has the effect of increasing the depth of the tissue to which the spectrophotometer is sensitive. Based on the hypothesis that the signal was not derived from the nerve itself, the prediction was made that signals would be similar for each source detector pair. Figure 4 shows an example of signals obtained from each source-detector pair in one of the animals. There was no statistically significant relationship between source-detector distance and signal amplitude.
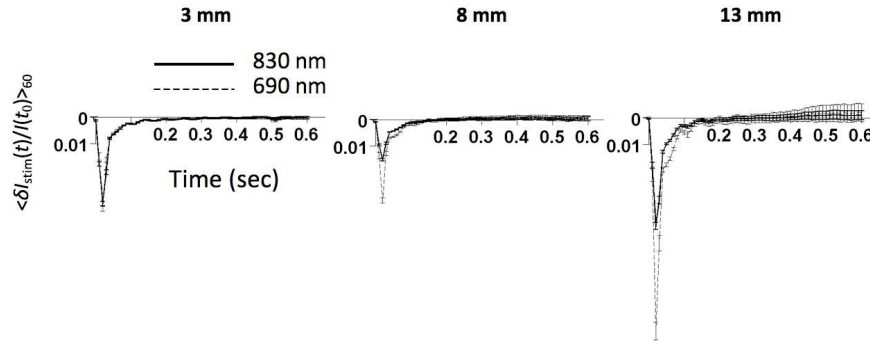

Fig. 4. Signals do not depend on the distance between source and detector. From left to right are examples of signals obtained from each source-detector separation in 1 rat. Across all 7 rats, there was no relationship between source-detector separation and response amplitude, suggesting that the response was not localized to an anatomical compartment with a specific depth from the surface of the tissue.

3.1.2 Effect of pharmacological and surgical neuromuscular block on evoked optical signals

In all 5 animals, a 0.2 mg/kg intra-arterial dose of Cisatracurium Besylate dramatically reduced, or completely eliminated the stimulation-induced signals. In 2 animals, the delivery of Cisatracurium Besylate completely eliminated statistically significant optical responses at each source detector separation, Fig. 5(a).

In 3 animals, optical responses were reduced by an order of magnitude though none-the-less remained statistically significant at several source-detector separations. Animals given an intravenous bolus of Cisatracurium at doses between 1.5 and 6 ED_{95} have been shown to begin spontaneously recovering after as little as 20 minutes [12]. In this study, boluses were being delivered intra-arterially; a route that could speed the clearance of the drug. Indeed, in one animal, following an approximately 15 minute washout period, the return of the plantar muscle CMAPs was associated with a dramatic return of the optical signal [Fig. 5 (c)]. This apparent dose-response relationship was later confirmed in a 6th animal in which signals were present following a 0.100 mg/kg dose but eliminated following a 0.6 mg/kg dose. This result suggests, though does not confirm, a correlation between the amplitude of the optical response and the percentage of recruited muscle fibers.
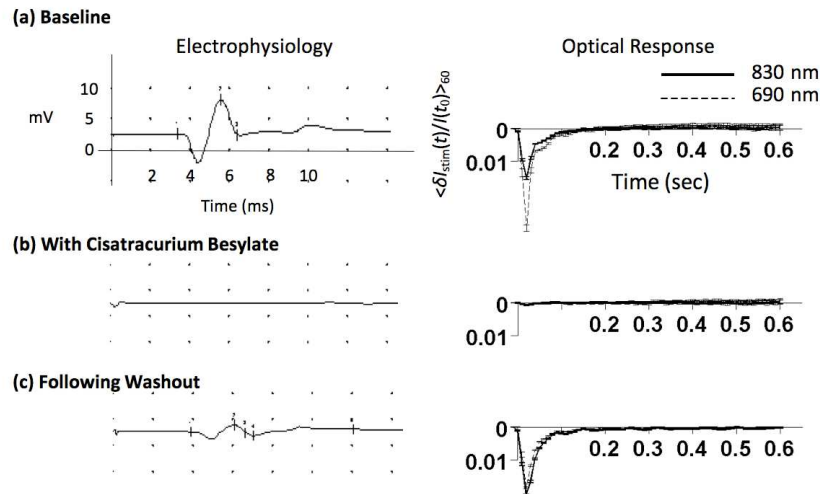
Fig. 5. The effect of Cisatracurium Besylate on signals generated in the rat. (a) Signals from the middle source-detector separation in one of the rats prior to delivery of the drug. (b) Optical traces from the same rat following drug delivery. (c) Following a 15 minute washout period, both the electrophysiological and optical response returned.

In an additional set of animals, the two divisions of the sciatic nerve (tibial and common peroneal) were surgically transected in the popliteal fossa. This manipulation produces the same functional disconnection of nerve from muscle while avoiding potential hemodynamic side affects associated with acetylcholine receptor blockade. In agreement with the pharmacological results, surgical disconnection of the nerve from the muscle eliminated nerve-stimulation induced optical responses at each source-detector separation.

3.2 Human subjects

3.2.1 Optical response to mixed nerve stimulation resulting in muscle motion

Figure 6 shows optical responses measured at the wrist of subject 2 during each stimulation condition involving a nerve that contained motor axons. The results in panels (a), (b) and (c) correspond to the experimental setups depicted in Fig. 2, panels (a), (b), and (c), respectively. Figure 6, panel (b) shows a supramaximal electrophysiological response measured in the APB and demonstrates that the entire muscle was recruited, which produced large amplitude motion of the thumb. The amplitude (~10%) of the corresponding optical response is 2 orders of magnitude larger than that of signals described previously [4], though the temporal and spectral features are comparable, suggesting a similar biological origin. Similar results were obtained during stimulation of both the ulnar nerve and the median nerve at the elbow [Fig. 6(a) and 6(c)]. While the median nerve does travel in the optically probed region, the ulnar nerve does not. However, both of these nerves do innervate muscles whose tendons are located in the distal forearm beneath the optical probe. In all subjects, stimulation under each of these three conditions resulted in large amplitude signals demonstrating that optical measurements at the wrist are sensitive to motion induced nerves both within and outside the region of optical interrogation.
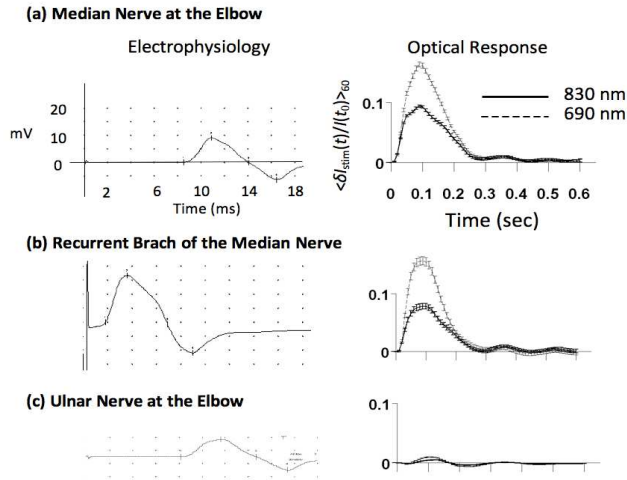
Fig. 6. Optical responses at the wrist during stimulation of mixed nerves in subject 2. (a) CMAP generated in APB (left) and the corresponding optical response (right) during stimulation of the median nerve at the elbow [c.f. Fig. 2, panel (a)]. (b) CMAP and corresponding optical trace during stimulation of the recurrent branch of the median nerve in the palm [c.f. Fig. 2, panel (b)]. (c) CMAP and corresponding optical response during stimulation of the ulnar nerve at the elbow [c.f. Fig. 2, panel (c)]. Differences in the latency-to-onset of the electrophysiological response between stimulation at the elbow and at the recurrent branch of the median nerve reflect the increased distance (~20 cm) over which the nerve impulse must travel before depolarizing the muscle.

3.2.2 Sensory nerve activation is insufficient to generate optical signals

Figure 7 shows the results from subject 2 during sensory nerve activation of the median nerve, medial antebrachial cutaneous nerve, and lateral antebrachial cutaneous nerve. The results shown in panels (a), (b), and (c) correspond to the experimental conditions depicted in Fig. 2, panels (d), (e), and (f), respectively. In each case, despite the presence of a robust electrical signal in the optically probed region, no optical response was detected. In all other subjects, no optical response was observed in any of the sensory stimulation conditions.

4. Discussion

The current study presents experimental evidence aimed at elucidating the biological origin of an intermediate optical signal elicited on stimulation of the peripheral nerve that supports the theoretical work presented in our companion paper [5]. The conclusions of that work suggest that motion of blood-containing structures within the optical field of interrogation, whether directly supplying or simply traveling with the nerve, could account for the signal currently under study, e.g., Fig. 8 shows photographs of the exposed sciatic nerve of the rat, which were taken during the surgical procedures required for the animal model used in this study. Whether by pharmacological, surgical, or anatomical means, signals are completely eliminated by functionally disconnecting the stimulated nerve from mechanical elements within the optically probed region. This proved true in both an animal model built in the Sprague-Dawley rat as well as in human subjects.
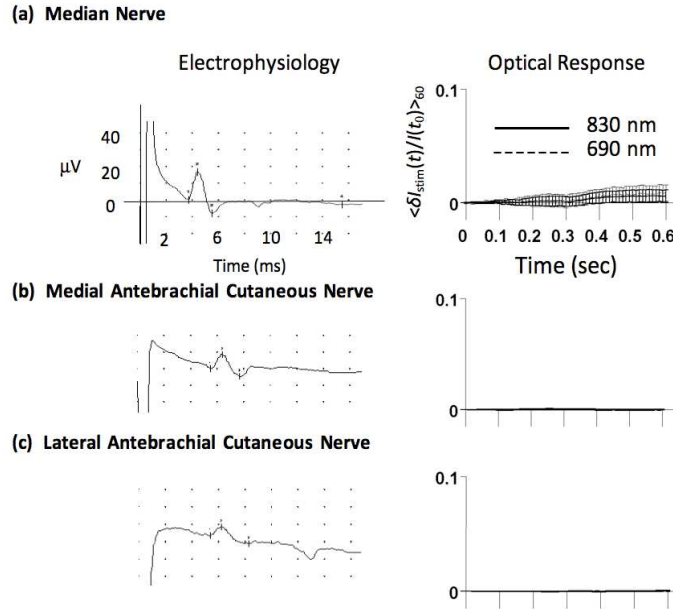
Fig. 7. Optical data during sensory nerve stimulation in subject 2. (a) Median nerve SNAP measured at the wrist during stimulation of the 2nd digit (top trace) and the corresponding optical data [c.f. Fig. 2(e) for the location of the probe]. (b) Medial antebrachial cutaneous SNAP and corresponding optical data [c.f. Fig. 2(f) for the location of the probe]. (c) Lateral antebrachial cutaneous SNAP and corresponding optical data [c.f. Fig. 2(g) for the location of the probe].

Despite large differences in amplitude, signals generated during motor stimulation have similar characteristics to those observed in previous studies [1,2,5]. Not only does their sign change depending on both the subject and the region of optical interrogation, but they are also wavelength dependent and have a timescale on the order of 100 ms, which has been shown to correspond to contraction times of intact human muscle [13]. In previous work, the stimulation site of the median nerve had been common palmar digital branch, which is located near the thenar group of muscles and the nerve that supplies them (the recurrent branch of the median nerve). Although care had been taken to stimulate at a level below the threshold of visible skin motion, it was noted that inadvertent stimulation of this recurrent branch could have resulted in muscle tensioning. This tensioning, mechanically coupled to the optically probed region via the soft tissues in the wrist, likely induced small optical signals. In the present study, the stimulator was moved to a site where sensory stimulation could not possibly result in motion, namely the proper digital branch of the median nerve. Even in the presence of a robust action potential measured at the wrist, no optical response could be elicited under these conditions. Moreover, signals that were obtained from direct stimulation of the recurrent branch of the median nerve demonstrate that thenar muscle activation, while not occurring in the region of optical interrogation, does induce a measurable optical response. Similar evidence of optical sensitivity to motion induced by a stimulation of a nerve outside the optically probed region presented in the ulnar nerve experiments. The ulnar nerve travels several centimeters medial to the median nerve in Guyon's tunnel as it enters the hand.
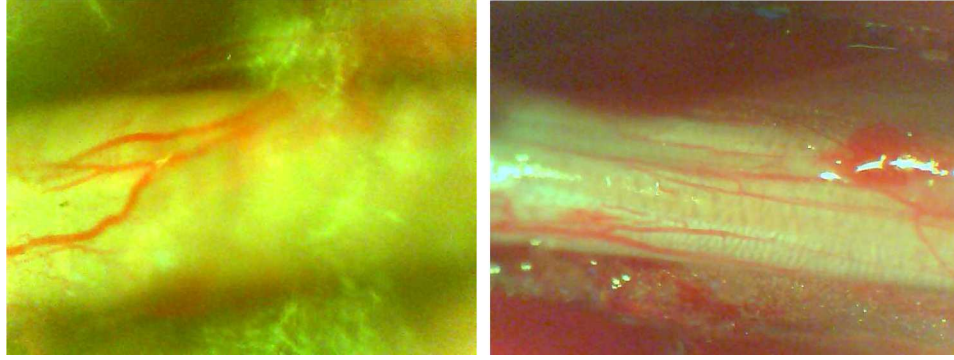
Fig. 8. Photographs taken through a dissecting microscope of the exposed sciatic nerve of the rat. Panels (a) and (b) are nerves from separate surgeries on different rats at different stages of the nerve exposure. (a) Vessels accompanying the nerve in the surrounding fascia. (b) With the fascia further dissected away, the epineurial plexus of arterioles that supply the nerve can be directly visualized.

In the rodent, the time to peak amplitude of nerve-stimulation induced signals were consistently faster than those obtained from human subjects. Their speed, however, is highly consistent with that of force-velocity measurements made in rat hind limb isolated muscle preparations, further corroborating the skeletal muscle hypothesis [14]. Moreover, by using a neuromuscular blocking agent or by surgically denervating lower limb muscles, the optical response was completely eliminated.

A proof of principle experiment (data not shown) in which both the kinetics of the optical signal and the muscle kinematics were concurrently measured demonstrated that muscle action as measured by direct movement of the muscle tendon were highly correlated. We currently speculate that the intermediate optical signal may provide a capacity to non-invasively monitor the electromechanical action of muscles on a millisecond time scale. This may have valuable clinical application if the features of this signal can be shown to be influenced by muscle fiber twitch kinematics that are altered at the structural molecular level in a variety of myopathic processes. It is also intriguing that metabolic derangements as well as mitochondrial disorders might alter the kinematics of muscle fibers at the millisecond time scale thus the optical signal may provide a clinical tool for the investigation of these important clinical diseases. Currently we are using both the animal and human models described in this paper in experiments that directly measure the muscle force and motion concurrently with the intermediate signal characteristics in an effort to elucidate of the dynamics and details of the intermediate optical signal as a biomarker for clinical muscular and neuromuscular physiology and pathbiology.

Acknowledgments